THE JOURNAL OF PHYSICAL CHEMISTRY B

Article

pubs.acs.org/JPCB

Photoluminescence and *trans* → *cis* Photoisomerization of Aminostyrene-Conjugated Phenylpyridine C^N Ligands and Their Complexes with Platinum(II): The Styryl Position and the Amino Substituent Effects

Che-Jen Lin, Yi-Hung Liu, Shie-Ming Peng, and Jye-Shane Yang*

Department of Chemistry, National Taiwan University, Taipei 10617, Taiwan

Supporting Information

ABSTRACT: The synthesis, electronic spectra, photochemical properties, and DFT calculations of four phenylpyridine (ppy)-derived C^N ligands and their cyclometalated [(C^N)Pt(II)(acac)] (C^N = *trans-n*-(4-NR_2-styryl)-2-phenylpyridine, where n = 3′ or 4 and R = Me or Ph, and acac = acetylacetonate) complexes are reported. The results allow one to address the effects of the styryl position (n = 3′ or 4) and the amino *N*-substituents (*N*-Me or *N*-Ph) on the photoluminescence and *trans* → *cis* photoisomerization quantum efficiencies (Φ_f and Φ_{tc}) of the free ligands and the Pt complexes. In general, the styryl position effect is more significant than the amino substituent effect. The relative Φ_f and Φ_{tc} values are distinct between the free ligands and the corresponding Pt complexes. However, the phenomenon of $\Phi_f + 2\Phi_{tc} \approx 1.0$ is observed for all cases in solutions at room temperature. This phenomenon is interpreted by the conventional one-bond-twist mechanism for photoisomerization, which is an activated process in S_1 but barrierless in T_1. We conclude that ca. 50% of the C=C bond torsion in the excited-state manifold leads to the *cis* isomer and the excited-state deactivations are dominated by fluorescence and *trans* → *cis* isomerization for both the ligands and the complexes.

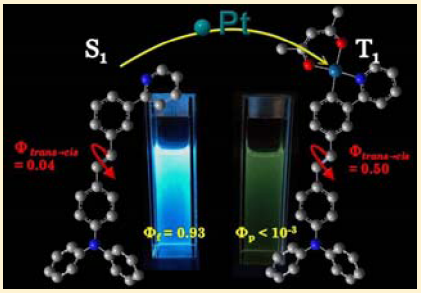

INTRODUCTION

Square-planar platinum(II) complexes exhibit rich photophysical and photochemical properties and have been extensively investigated as light-emitting,[1−10] photochromic,[11,12] and sensory[13−19] materials. The lowest triplet excited state (T_1) generally dominates the observed properties due to efficient intersystem crossings from the lowest singlet excited state (S_1) to the triplet states (T_1 or T_n). The nature of the T_1 state strongly depends on the ligands and could be of predominant metal-centered (MC), ligand-centered (LC), metal-to-ligand charge-transfer (MLCT), or ligand-to-metal charge-transfer (LMCT) character. A variety of cyclometalating ligands[1,3,6−10,20−22] have been developed to enhance the photoluminescence property by raising the nonemissive MC d-d state above the emissive LC or MLCT states. Among them, the bidentate C^N ligands such as 2-phenylpyridine (ppy) and its derivatives have attracted much attention.[20,22,23] Optical properties of the ppy-cyclometalated Pt complexes can be readily tuned by introducing substituents of desired electronic and steric properties to the phenyl and/or the pyridyl rings.

trans-Stilbene and its analogues are important chromophores in many organic and organometallic materials for applications in nonlinear optics,[24−29] light-emitting diodes,[30−36] photochemical molecular devices,[37,38] and optical sensors.[39−45] The wide application of *trans*-stilbenes stems from its feasible synthesis, suitable optical bandgap, and intriguing photochemical activities, particularly the *trans* → *cis* photoisomerization. According to the one-bond-twist (OBT) mechanism adopted by the parent *trans*-stilbene (Figure 1),[46−51] torsion of the central C=C bond can occur in S_1 and/or T_1 and reaches a

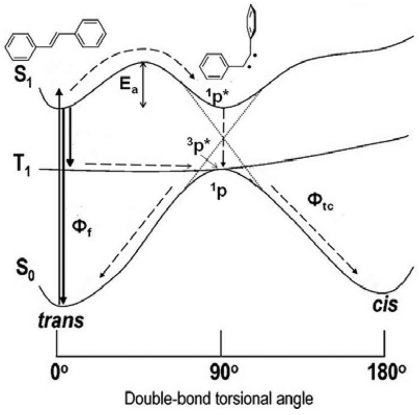

Figure 1. Simplified potential energy surface diagram for the lowest electronic states of stilbene. The dash arrows show the *trans* → *cis* photoisomerization pathways of the one-bond-twist (OBT) mechanism.

Received: May 21, 2012
Revised: June 21, 2012
Published: July 10, 2012

 © 2012 American Chemical Society dx.doi.org/10.1021/jp304893c | *J. Phys. Chem. B* 2012, 116, 8222−8232

conical intersection at a state of nearly perpendicular geometry between the two attached phenyl rings ($^1p^*$ or $^3p^*$). Internal conversion of $^1p^*$ and/or intersystem crossing of $^3p^*$ results in the transition state (^1p) of trans−cis interconversion on the ground-state (S_0) potential energy surface (PES). Because of the small energy difference between the *trans* and *cis* isomers, the driving force from ^1p to either isomer is similar. Consequently, the determined *trans* → *cis* isomerization quantum yield (Φ_{tc}) corresponds approximately to half of the quantum efficiency for the C═C torsion (i.e., $\Phi_{torsion} \approx 2\Phi_{tc}$). Photoisomerization via the OBT mechanism has been demonstrated for many other *trans*-stilbenes, including *trans*-aminostilbenes[52−55] and *trans*-stilbazoles.[56,57] Thus, the sum of $\Phi_f + 2\Phi_{tc}$, where Φ_f is the fluorescence quantum yield, could be a useful parameter for judging whether decay channels other than fluorescence and the C═C torsion are important for these systems. Specifically, a value of $\Phi_f + 2\Phi_{tc}$ near 1.0 reveals that the excited decay is mainly due to fluorescence and the C═C torsion, but a value much less than 1.0 is an indication of the presence of new decay channels. Examples of the latter have been reported for some *trans*-aminostilbenes and *trans*-stilbazoles under certain conditions due to the formation of a twisted intramolecular charge-transfer (TICT) state[58] and to the n,π^*-mediated internal conversions,[57] respectively.

Pt(II) complexes containing a *trans*-stilbene or *trans*-stilbenoid moiety in the ligands have been reported.[59−63] The common feature of these complexes is weak photoluminescence in fluid solutions at room temperature. However, the origin of luminescence quenching is ligand-dependent. For the complexes $[L_2Pt(—C\equiv C—t\text{-St})_2]$ (L = phosphine ligand and *t*-St = *trans*-4-stilbene) reported by Shanze et al.[59] and [(C^N)Pt(acac)] (C^N = *trans*-4-(4-R-styryl)-2-phenylpyridine and acac = acetyl- acetonate) reported by Williams et al.,[60] the low phosphorescence quantum yield ($\Phi_p < 0.01$) was attributed to efficient *trans* → *cis* isomerization of the stilbenoid olefins, disregarding the T_1 state being LC or MLCT character. In contrast, the weak or no photoluminescence of complexes [(N^C^N)PtCl] (N^C^N = *trans*-2,6-$(CH_2NMe_2)_2$- 4′-R-stilbene) reported by van Koten et al.[61] was ascribed mainly to Pt-induced internal conversions. Very recently, Baik and Wang reported a boron-containing *trans*-stilbenoid ligand that undergoes *trans* → *cis* isomerization in the free ligand but not after complexation with Pt(II).[63] This was explained with a low-lying MLCT state of no isomerization activity. Evidently, more studies are required to understand the relationship between the structure of *trans*-stilbenoid ligands and their photoisomerization activity upon metalation with Pt(II).

Following our long-term interest in the photochemistry of *trans*-aminostilbenes,[54,55,58,64−66] we have investigated new bidentate C^N ligands (compound series **L**) and their cyclometalated Pt(II) complexes [(C^N)Pt(acac)] (compound series **C**), in which both the moieties of ppy and *trans*-4-aminostilbene or *trans*-4,4′-aminostilbazole are present (Chart 1). Our objectives in this work are to investigate the styryl position effect (compound series **1** vs **2**) and the *N*-phenylamino conjugation effect (compound series **Ph** vs **Me**) on the photochemical behavior of the free ligands and the Pt complexes. The structural design was in part inspired by the study of Williams and co-workers, in which a system resembling **C1-Me** (i.e., **C1-Et**) was reported to possess a predominantly intraligand charge transfer (ILCT) character in both S_1 and T_1.[60] While the *trans* → *cis* isomerization activity of **C1-Et** was well demonstrated with NMR spectroscopy, the Φ_{tc} data were

Chart 1

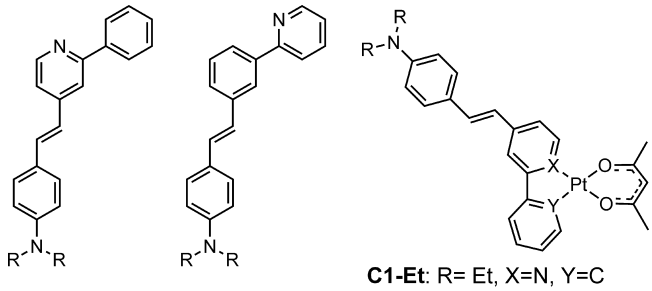

not reported. In addition, *N*-phenyl substitution of *trans*-4-aminostilbenes could lead to a dramatic enhancement in fluorescence by suppressing the C═C bond torsion in S_1 (referred to as the amino conjugation effect).[54,65] However, its influence in T_1 and in *trans*-4,4′-stilbazoles remains unknown. The results reported herein show that both **C1** and **C2** possess an ILCT nature for their T_1 states, and the styryl position imposes a larger effect than the amino *N*-phenyl substituents on the absorption and emission spectra of both the ligands and complexes. The emission-enhanced amino conjugation effect is observed for both **L1** and **L2** but not for their Pt complexes. All the compounds exhibit the phenomenon of $\Phi_f + 2\Phi_{tc} \approx 1.0$, indicating that their nonradiative decay is dominated by the C═C torsion.

RESULTS AND DISCUSSION

Molecular Structure. The target ligands were prepared via the Heck reaction[67,68] with bromosubstituted 2-phenylpyridines and aminostyrenes, and the Pt complexes were synthesized employing the two-step protocol reported by Thompson et al. with the ligands, K_2PtCl_4, and acetylacetone as starting materials.[23] Detailed synthetic scheme (Scheme S1, Supporting Information) and compound characterization data are provided as Supporting Information. All four Pt complexes are air-stable yellow-orange solid at ambient conditions.

Single crystals of **L2-Ph** and **C2-Ph** suitable for X-ray crystallographic studies were obtained from slow evaporation of solvents at ambient conditions. The crystal structures are supplied in the Supporting Information (Figure S1), and selected structural data for the amino group and the ppy moiety are listed in Table 1. There are two independent conformers of **L2-Ph** in each asymmetric unit, differing in the orientation of the propeller arrangement of the three *N*-phenyl rings and in the dihedral angle (χ_{py}) between the two rings of the ppy moiety (2° vs 18°). However, the dihedral angles (χ_{amino}) between the amino *N*-phenyl rings and the stilbene *c* ring (ca. 30°), the sum of the bond angles (θ) about the amino nitrogen (ca. 360°), the stilbene-amino C−N bond length (d_{CN} = 1.43 Å), and the phenyl-pyridine C−C bond length (d_{CC} =1.48 Å) are similar or the same for both conformers. In the case of **C2-Ph**, there is only a single conformation in the crystal. Compared to the free ligand **L2-Ph**, the θ, d_{CN}, and d_{CC} are not much changed, but the χ_{amino} (38 and 48°) is significantly increased and the ppy moiety is nearly coplanar (χ_{py} = 1°). The square-planar geometry around Pt is characterized by similar Pt−C (d_{PtC}) and Pt−N (d_{PtN}) bond lengths (ca. 2.0 Å) and by a C−Pt−N bond angle (θ_1) of ca. 81° and the other three bond

dx.doi.org/10.1021/jp304893c | J. Phys. Chem. B 2012, 116, 8222−8232

Table 1. Selected Structural Data and Dipole Moments for the X-ray Single Crystal and DFT-Optimized Structures of the Ligands and Complexes[a,b]

compound	θ (deg)	χ_{amino} (deg)	χ_{py} (deg)	d_{CN} (Å)	d_{CC} (Å)	d_{PtC} (Å)	d_{PtN} (Å)	θ_1 (deg)	μ (D)
L2-Ph-crystal[c]	360.0	30.1/33.7	1.5	1.43	1.48				
	359.8	23.2/39.0	18.0	1.43	1.48				
C2-Ph-crystal	359.9	38.1/48.0	0.6	1.41	1.46	1.96	1.99	81.4	
L1-Me-DFT	358.7		20.1	1.38	1.49				6.57
L2-Me-DFT	357.1		20.6	1.39	1.49				4.25
L1-Ph-DFT	360.0	44.1/45.5	20.5	1.41	1.49				4.29
L2-Ph-DFT	360.0	42.2/43.2	20.2	1.42	1.49				2.13
C1-Me-DFT	360.0		0.0	1.38	1.46	1.98	2.02	81.0	8.21
C2-Me-DFT	360.0		0.0	1.38	1.46	1.98	2.02	81.0	2.89
C1-Ph-DFT	360.0	44.9/45.8	0.1	1.41	1.46	1.98	2.02	81.0	6.08
C2-Ph-DFT	360.0	40.6/42.1	0.2	1.41	1.46	1.98	2.02	81.0	3.31

[a]Compounds labeled with crystal or DFT correspond to X-ray crystal or DFT-optimized structures, respectively. [b]See below for the structural notations. [c]Two independent conformers.

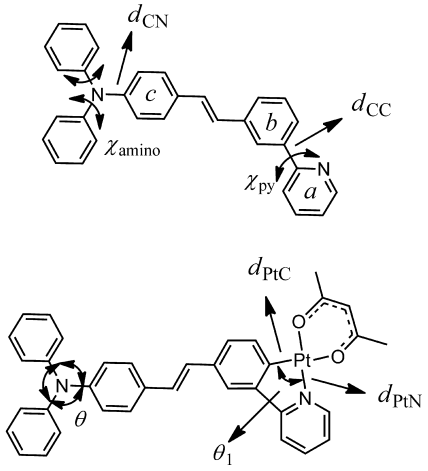

angles of ca. 92°. More structural details are provided in Table S1 in the Supporting Information.

To gain a complete picture of the structures, we have performed DFT calculations with the B3LYP[69−71]/6-31G(d,p) method for the ligands and with the Cam-B3LYP[72]/GenECP (6-31G(d,p) for C, H, N, O and SDD[73] for Pt) method for the Pt complexes. The calculated structural data are listed in Table 1. For the ligands, the difference in the *N*-substituents (Me or Ph) or in the styryl position has little influence on the ppy moiety ($\chi_{py} \approx 21°$ and $d_{CC} = 1.49$ Å). However, **L1-Ph** and **L2-Ph** display slightly larger d_{CN} and θ than **L1-Me** and **L2-Me**. The difference in d_{CN} might be attributed to a different degree of steric congestion about the N atom, and the difference in θ is known to be a character of varied conjugation interactions. For **L2-Ph**, the DFT-calculated structural parameters agree well with those in the crystal, except for χ_{amino}. The smaller χ_{amino} values in the crystal structures might reflect some molecular packing effects. For the Pt complexes, all four systems display an sp^2-hybridized amino N (i.e., $\theta = 360°$), coplanar ppy moiety ($\chi_{py} = 0°$), and square-planar conformation around the Pt atom. There is an excellent agreement between the calculated and the X-ray crystal structures of **C2-Ph** (structural details are shown in Table S1, Supporting Information).

UV−vis Absorption Spectra. UV−vis absorption spectra of the ligands and the Pt complexes in dichloromethane (DCM) are shown in Figure 2, and the spectral data in hexane (Hex), DCM, and acetonitrile (MeCN) are listed in Table 2. The absorption maxima (λ_{abs}) of the ligands are in the order **L1-Ph** > **L1-Me** > **L2-Ph** > **L2-Me** in DCM and MeCN.

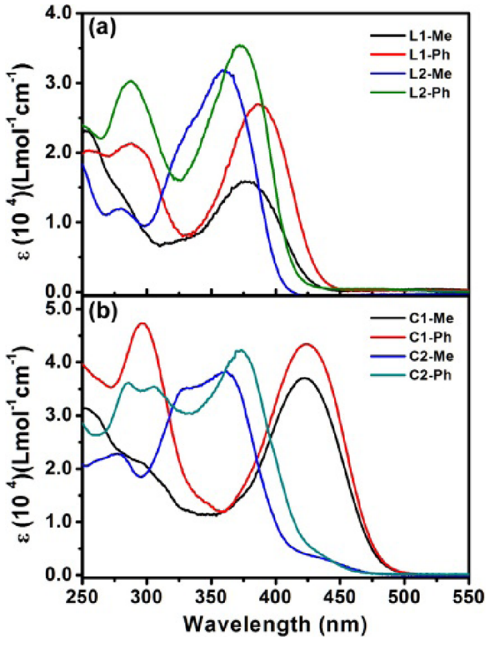

Figure 2. UV−vis absorption spectra of (a) the ligands and (b) the Pt complexes in DCM.

Evidently, the styryl position causes a larger effect than the amino *N*-substituents on the optical transition energy. Since the phenyl group of ppy in **L1-Ph** and **L1-Me** is cross-conjugated (meta connectivity) to the aminostyryl group, the spectra of

dx.doi.org/10.1021/jp304893c | J. Phys. Chem. B 2012, 116, 8222−8232

Table 2. Maxima of Absorption (λ_{abs}) and Fluorescence (λ_f), Extinction Coefficients (ε), Fluorescence-Band Half-Width ($\Delta\nu_{1/2}$), and Stokes Shifts ($\Delta\nu_{st}$) of the Ligands and the Pt Complexes in Solutions

compound	solvent	λ_{abs} (nm)	ε (L mol^{-1} cm^{-1})	λ_f[a] (nm)	$\Delta\nu_{1/2}$ (cm^{-1})	$\Delta\nu_{st}$[b] (cm^{-1})
L1-Me	Hex	363	38000	400 (424)	2986	2548
	DCM	376	16000	482	2905	5849
	MeCN	375	25000	502	3002	6746
L1-Ph	Hex	378	31000	417 (444)	2610	2474
	DCM	386	27000	500	3316	5907
	MeCN	381	34000	523	3747	7126
L2-Me	Hex	349	33000	389 (410)	3311	2946
	DCM	361	32000	457	3905	5819
	MeCN	356	31000	516	5252	8710
L2-Ph	Hex	366	45000	401 (424)	2510	2385
	DCM	372	36000	456	3404	4952
	MeCN	366	40000	471	3799	6091
C1-Me	Hex	411	42000			
	DCM	422	37000	541	3526	5212
	MeCN	420	40000			
C1-Ph	Hex	417	49000			
	DCM	424	43000	568	3694	5979
	MeCN	416	37000			
C2-Me	Hex	334	44000			
	DCM	362	38000	(487) 516	2990	8244
	MeCN	360	42000			
C2-Ph	Hex	375	51000			
	DCM	373	42000	451 (486/516)	4298	4637
	MeCN	370	50000			

[a]The shoulders are given in parentheses. [b]$\Delta\nu_{st} = \nu_{abs} - \nu_f$.

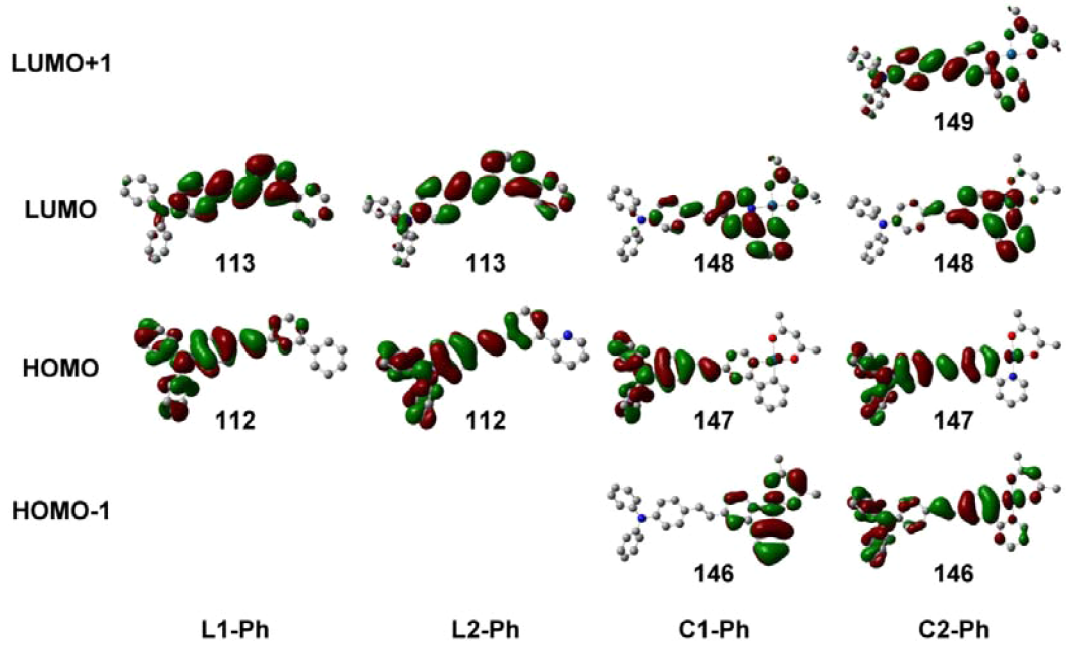

Figure 3. Frontier molecular orbitals of **L1-Ph**, **L2-Ph**, **C1-Ph**, and **C2-Ph**.

these two systems can be approximately considered as a simple summation of the two localized chromophores of *trans*-4-aminostilbazole and ppy. Likewise, the two localized chromophores in **L2-Ph** and **L2-Me** are *trans*-4-aminostilbene and ppy. The λ_{abs} of **L2-Ph** (366 nm) and **L2-Me** (349 nm) in hexane are similar to those of *trans*-4-(*N*,*N*-diphenylamino)-stilbene (362 nm)[54] and *trans*-4-(*N*,*N*-dimethylamino)stilbene (347 nm),[54] respectively. Evidently, the long-wavelength absorption bands of **L1** and **L2** are characterized by the *trans*-aminostilbazole and the *trans*-aminostilbene chromophores, respectively. As pyridine is a stronger electron acceptor than benzene, it is expected that *trans*-aminostilbazoles possess a larger charge-transfer (CT) character than *trans*-aminostilbenes.[57] This is consistent with the larger molecular dipoles (Table 1) and λ_{abs} values (Table 2) for **L1** vs **L2** of the same *N*-substituents. Regarding the amino *N*-substituent effect, the **Ph**

dx.doi.org/10.1021/jp304893c | J. Phys. Chem. B 2012, 116, 8222−8232

systems exhibit red-shifted and hyperchromic absorption spectra as compared to the **Me** systems. This reflects an extended conjugation of the system by the *N*-phenyl groups, as previously demonstrated for simple aminostilbenes.[54] The styryl position effect on the long-wavelength absorption band is further enhanced upon metalation with Pt(II). The absorption maxima are red-shifted by 40 nm for **C1** vs **L1** (Figure 2b). In contrast, **C2** displays nearly the same absorption maxima as **L2** (Table 2), although a shoulder emerged at the red side of the spectrum for both **C2** complexes. Also worth noting is the same long-wavelength onset of the absorption spectra for the couple of **C1-Me** and **C1-Ph** (~500 nm) and that of **C2-Me** and **C2-Ph** (~475 nm). It appears that the optical transition energy of the complexes is rather insensitive to the *N*-substituents.

To gain insights into the nature of electronic transitions of these π-systems, we have carried out TDDFT calculations with the DFT-optimized molecular structures. Detailed frontier molecular orbitals (FMOs) and information about configuration interactions and oscillator strength (f) for S_1–S_3 are shown in Figures S2 and S3 and Table S2 in the Supporting Information. Selected FMOs and data are shown in Figure 3 and Table 3. The calculated transition energies agree qualitatively well with the relative order of the experimentally observed absorption maxima. The following discussion is based on the **Ph** systems, as the **Me** systems have similar features. For the ligands, the S_1 state is mainly due to the HOMO → LUMO transition. The HOMO is located on the aminostilbene moiety for both **L1-Ph** and **L2-Ph**, and the LUMO is mainly on the stilbazole moiety for **L1-Ph** and on the stilbene moiety for **L2-Ph** (Figure 3). These FMOs echo the above conclusion based on their λ_{abs} values that the long-wavelength electronic transition for **L1** and **L2** is characterized by the *trans*-aminostilbazole and *trans*-aminostilbene chromophores, respectively. For the Pt complexes, the S_1 state is also dominated by the HOMO → LUMO configuration. Whereas the S_2 state is HOMO-1 → LUMO for **C1-Ph**, it is HOMO → LUMO+1 for **C2-Ph**. Since the Pt atom plays a relatively minor role in these FMOs, both the S_1 and S_2 states have a prominent ILCT character. This is consistent with the assignment of a substantial ILCT character for **C1-Et** by the Williams group.[60] Nevertheless, the Pt atom possesses some electron density in the LUMO of **C2-Ph** and in the LUMO+1 of **C1-Ph**. This might explain the lower oscillator strength for the S_1 state of **C2-Ph** vs **C1-Ph** and for the S_2 state of **C1-Ph** vs **C2-Ph**. These features highlight the styryl position effect on the optical properties of the ligands and the Pt complexes.

To further support the ILCT assignment for the absorption bands of the Pt complexes, we have investigated the titration spectra of the ligands with proton (HCl) and zinc(II) ($Zn(ClO_4)_2$) in MeCN. Specifically, a dominant ILCT transition in the Pt complexes suggests that the Pt atom functions mainly as a Lewis acid. Similar spectral responses would thus be expected for the ligands upon reacting with other Lewis acids such as proton and Zn(II), even though these Lewis acids cannot induce any low-lying MLCT transition. Indeed, the titration spectra resemble the spectral changes upon metalation with Pt for **L1-Me** and **L1-Ph** (Figure 4). The observation of a larger red shift induced by Zn(II) vs Pt complexation might be a consequence of the relatively larger Lewis acidity and electron affinity of zinc vs platinum.[74,75] The titration spectra for **L2-Ph** also resemble the spectrum of **C2-Ph**. The little effect of the Lewis acids on the long-wavelength absorption band of **L2-Ph**, which is dominated by the *trans*-4-aminostilbene (vide supra), could be understood by the meta-conjugated pyridyl group to the aminostyryl group so that the two N centers have little resonance interactions. Nevertheless,

Table 3. TDDFT-Calculated Electronic Transition Energy (ΔE), Oscillator Strength (f), and Description and Percentage of Configuration Interactions for the Ligands and Complexes

compd	excited state	ΔE (nm)	f	description	percentage
L1-Me	S_1	340	1.4929	80 → 81	85%
L1-Ph	S_1	348	1.5495	112 → 113	78%
L2-Me	S_1	329	1.4630	80 → 81	76%
L2-Ph	S_1	340	1.5475	112 → 113	76%
C1-Me	S_1	370	1.7091	115 → 116	87%
	S_2	337	0.0378	114 → 116	71%
C1-Ph	S_1	374	1.7780	147 → 148	79%
	S_2	341	0.0362	146 → 148	66%
C2-Me	S_1	365	0.3312	115 → 116	64%
	S_2	323	1.6839	115 → 118	61%
C2-Ph	S_1	359	0.6443	146 → 148	30%
				147 → 148	51%
	S_2	333	1.3402	147 → 149	65%

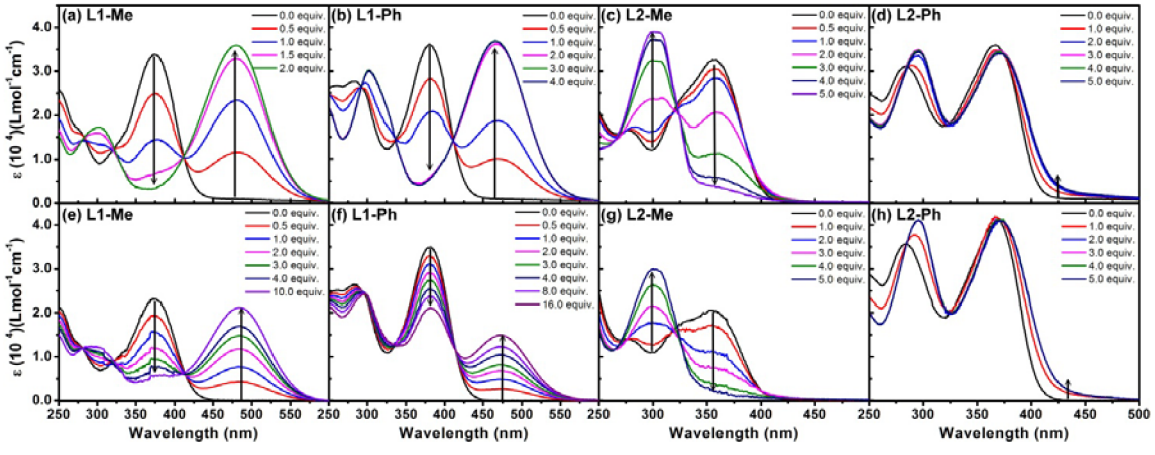

Figure 4. The absorption titration spectra of **L1** and **L2** systems with HCl (a–d) and with $Zn(ClO_4)_2$ (e–f) in MeCN.

dx.doi.org/10.1021/jp304893c | J. Phys. Chem. B 2012, 116, 8222–8232

the shoulder at the onset of the **L2-Ph** titration spectra is less intense than that of **C2-Ph**. This could have more than one possible origin. One possible origin is the different conformation of the ppy moiety, which is more planar in **C2-Ph** than in **L2-Ph** (Table 1). A more planar π-scaffold could enhance the probability of amino → pyridyl CT across the *meta*-phenylene linker.[76] An alternative explanation is the presence of minor amino → dπ*(Pt) LMCT character for **C2-Ph** but not for the protonated ligands. It should be noted that the protonation acts only on the pyridyl group but the cyclometalation involves both the phenyl and the pyridyl rings of ppy. The Pt−Ph bonding in **C2** might facilitate the LMCT interactions. However, it is less important in **C1**, as the phenyl ring is meta to the *trans*-aminostilbazole chromophore. In contrast, the **L2-Me** titration spectra differ from the spectrum of **C2-Me** to a significant extent and exhibit a blue shift of the absorption band (356 → 301 nm). As depicted in Scheme 1a,

Scheme 1. (a) Protonation of the Dimethylamino Group in L2-Me and (B) Resonance Structure of the Pyridinium Form of L1-Me

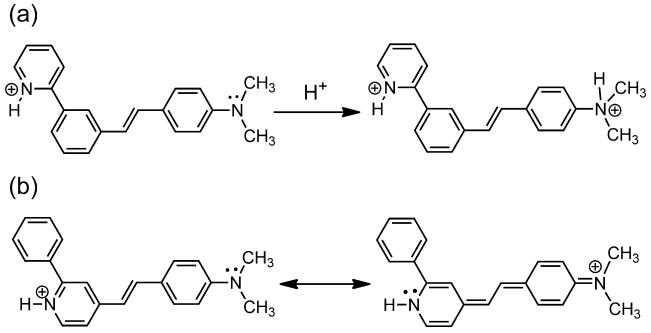

the blue shifts could be attributed to interactions of the Lewis acid with both the pyridyl (pK_a = 5.23) and dimethylamino N atoms (pK_a = 5.07).[77] Protonation or Zn(II) coordination of the amino N significantly reduces the push−pull character of the aminostilbene chromophore and thus leads to a blue-shifted CT band. Protonation of the amino N in **L2-Ph** is unfavorable due to the weak basicity of triarylamines (pK_a too small to measure). Protonation of the dimethylamino group in **L1-Me** is also unfavorable, unless in large excess of HCl (see Figure S4, Supporting Information), due to the resonance interactions of the pyridinium precursor shown in Scheme 1b.

Excited-State Behavior of the Ligands. All four ligands exhibit fluorescence upon photoexcitation. Figure 5 illustrates their fluorescence spectra in hexane, DCM, and MeCN. The fluorescence band half-width ($\Delta\nu_{1/2}$) and the size of Stokes shifts ($\Delta\nu_{st}$) in MeCN are significantly larger than those in hexane, which is consistent with a CT character of the S_1 state (Table 2). The solvatofluorochromic shift, as defined by the energy difference between the fluorescence 0−0 band in hexane and the peak maximum in MeCN, is in the order **L2-Me** (6327 cm^{-1}) > **L1-Me** (5080 cm^{-1}) ~ **L1-Ph** (4860 cm^{-1}) > **L2-Ph** (3706 cm^{-1}). This order might qualitatively reflect the relative dipole moment and the CT character of their S_1 states. As indicated by the TDDFT calculations (vide supra), the HOMO → LUMO transition in **L2-Me** involves CT from the amino donor to the pyridyl acceptor. Since the donor and acceptor are meta-connected through the ppy phenyl group, the excited state is referred to as a meta-CT state (Figure 6). However, such a meta-CT character is much weaker in **L2-Ph**, as the

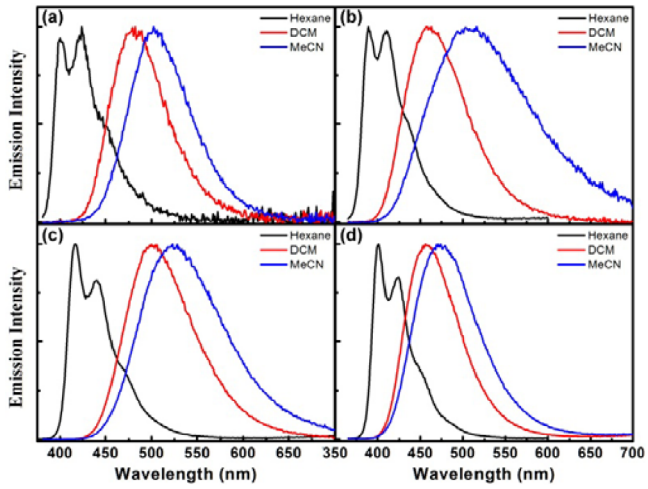

Figure 5. Normalized fluorescence spectra of (a) **L1-Me**, (b) **L2-Me**, (c) **L1-Ph**, and (d) **L2-Ph** in hexane (black), DCM (red), and MeCN (green) (λ_{ex} = 355 nm for **L2-Me** and λ_{ex} = 371 nm for the others).

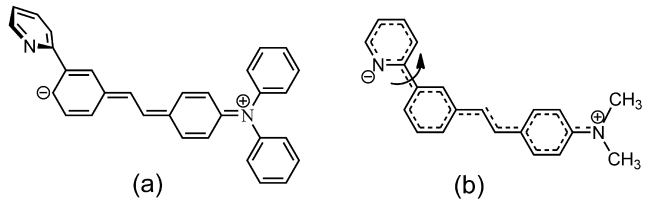

Figure 6. Schematic representations of the (a) aminostilbene-localized and (b) meta-delocalized charge transfer S_1 state for **L2-Ph** and **L2-Me**, respectively. The curved arrow in part b denotes the presence of a distribution of the pyridyl-phenyl dihedral angle in **L2-Me**.

pyridyl group plays a relatively minor role in LUMO. This might infer that the excited state is largely localized within the aminostilbene chromophore. In contrast, the amino donor and the pyridyl acceptor are para-conjugated within the aminostilbazole chromophore of **L1-Me** and **L1-Ph**, and there is negligible participation of the ppy phenyl ring in LUMO. Therefore, their excited state is essentially characterized by the *trans*-aminostilbazole chromophore and referred to as a para-CT state. Our previous studies[65,66] on *trans*-aminostilbenes have shown that a meta-CT state possesses a larger extent of charge separation than a para-CT state. In addition, the distance of charge separation is larger in the meta-CT state of **L2-Me** than the para-CT state of **L1-Me** and **L1-Ph**. These two factors might account for a larger excited-state dipole moment for **L2-Me** than the two **L1** systems. Having a para-CT character for **L1-Me**, **L1-Ph**, and **L2-Ph**, their relative dipole moment is determined by the push−pull character of the chromophore, which is larger for aminostilbazole (**L1-Me** and **L1-Ph**) than aminostilbene (**L2-Ph**). Although the dimethylamino group is a stronger donor than the diphenylamino group, the latter has a larger dynamic volume. Consequently, the solvatofluorochromic shifts are similar for **L1-Me** and **L1-Ph**.

All four ligands undergo *trans* → *cis* isomerization upon irradiation. Figure 7 shows the hypso- and hypochromic shifts of their absorption spectra upon prolonged irradiation as expected for the formation of less planar *cis* isomers. The presence of isosbestic points in each case indicates one-to-one conversion between the *trans* and *cis* isomers.

dx.doi.org/10.1021/jp304893c | J. Phys. Chem. B 2012, 116, 8222−8232

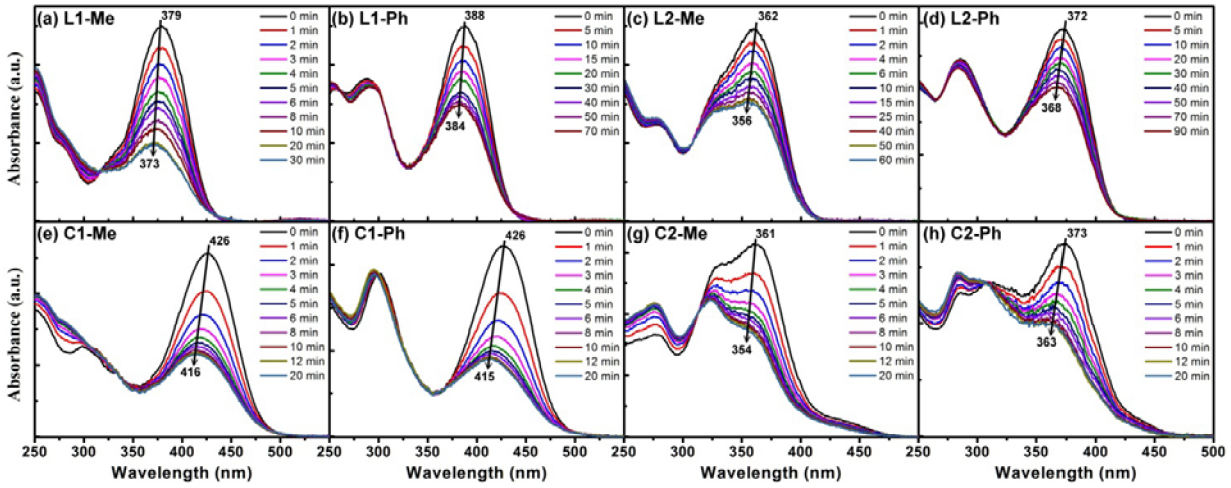

Figure 7. Absorption spectra of the ligands and Pt complexes in DCM recorded at different irradiation times at the red-edge of their long-wavelength absorption bands. The excitation wavelength for **L1**, **L2**, **C1**, and **C2** systems are 430, 410, 470, and 430 nm, respectively.

Table 4. Quantum Yields for Fluorescence (Φ_f) and Photoisomerizaiton (Φ_{tc}), Fluorescence Decay Times (τ_f), and Rate Constant for Fluorescence Decay (k_f) and Nonradiative Deacy (k_{nr}) in Solution at 298 K and in a MTHF Glass at 77 K

compd	solvent	Φ_f	Φ_{tc}[a]	τ_f[b] (ns)	k_f (10^8 s^{-1})	k_{nr} (10^8 s^{-1})
L1-Me	Hex	0.03	0.50	~0.1		
	DCM	0.09	0.51	0.2	4.1	41.4
	MeCN	0.13	0.47	0.4	3.3	22.3
L1-Ph	Hex	0.77	0.14	1.5	5.0	1.5
	DCM	0.92	0.03	2.6	3.5	0.3
	MeCN	0.95	0.02	3.6	2.7	0.1
L2-Me	Hex	0.19	0.36	0.6	3.3	14.2
	DCM	0.24	0.41	1.8 (77%), 0.3 (23%)	0.2[c]	0.5[c]
	MeCN	0.33	0.31	6.2 (83%), 2.9 (17%)	0.1[c]	0.1[c]
L2-Ph	Hex	0.68	0.25	1.3	5.1	2.4
	DCM	0.93	0.04	2.6	3.7	0.3
	MeCN	0.95	0.08	3.4	2.8	0.2
C1-Me	Hex	$<10^{-3}$	0.43			
	DCM		0.42 (0.47)			
	MeCN		0.46			
C1-Ph	DCM	$<10^{-3}$	0.41 (0.55)			
	MeCN		0.42			
C2-Me	Hex	$<10^{-3}$	0.50			
	DCM		0.52			
	MeCN		0.51			
C2-Ph	DCM	$<10^{-3}$	0.44			
	MeCN		0.50			

[a]Solutions were N_2-outgassed. Values in parentheses are determined with degassed solutions through three freeze−pump−thaw cycles. The hexane solutions contain 10% THF for the solubility reason. [b]The value of lifetime was determined with excitation and emission wavelengths around the spectral maxima. [c]The rate constant was determined using an averaged lifetime.

The data of Φ_f and Φ_{tc} of all four ligands in hexane, DCM, and MeCN are reported in Table 4. The **Ph** systems exhibit significantly larger Φ_f and lower Φ_{tc} than the corresponding **Me** systems in the same solvent. Such an *N*-Ph vs *N*-Me substituent effect on Φ_f and Φ_{tc} has been observed for many *trans*-aminostilbenes and attributed to an increase in the C═C torsion barrier (E_a) in S_1 (Figure 1).[54] The large *N*-substituent and solvent effects on Φ_{tc} suggest that photoisomerization of the free ligands likely occurs in S_1 and the amino conjugation effect found for *trans*-4-aminostilbenes also applies to *trans*-4,4′-aminostilbazoles. The aminostyryl position effect on Φ_f and Φ_{tc} is small in the **Ph** systems but is moderate in the **Me** systems. The lower Φ_f and higher Φ_{tc} for **L1-Me** vs **L2-Me** indicates that the former has a lower barrier for the C═C torsion.

The phenomenon of $\Phi_f + 2\Phi_{tc} \sim 1.0$ is present for all four cases. Under the OBT mechanism for *trans* → *cis* photoisomerization and the assumption of equal partition probability of the intermediates $^1p^*$ to the *trans* and the *cis* isomers, we might conclude that fluorescence and the nonradiative C═C bond torsion compete with one another and dominate the decay of the electronically excited states. For comparison, *trans*-4-stilbazole was reported to have an additional nonradiative

dx.doi.org/10.1021/jp304893c | J. Phys. Chem. B 2012, 116, 8222−8232

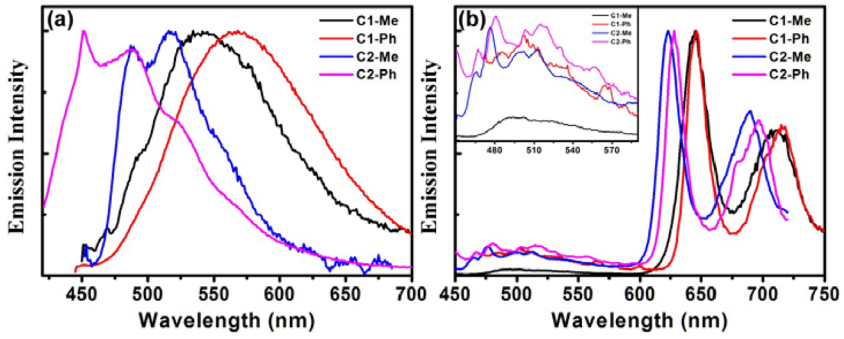

Figure 8. Emission spectra of **C1-Me** (black), **C1-Ph** (red), **C2-Me** (blue), and **C2-Ph** (purple) in (a) DCM at room temperature and (b) a MTHF glass at 77 K with the higher energy emission band amplified (inset).

decay channel associated with the n,π^* state on the basis of $\Phi_f + 2\Phi_{tc} = 0.74$ in hexane.[57] Evidently, introduction of an amino group at the 4′ position of *trans*-4-stilbazole has reduced the n,π^*-mediated nonradiative decay.

The room-temperature fluorescence decays can be well fitted by single-exponential functions in all cases, except for the decays of **L2-Me** in DCM and MeCN that require biexponential fitting parameters. A biexponential population decay could arise from two distinct emitting populations or from a Gaussian distribution of decay times associated with a distribution of conformations.[78] Since the CT excited state of **L2-Me** is associated with the meta-conjugated pyridyl group (vide supra) and meta-conjugated donor−acceptor systems tend to have a larger distribution of the torsion angles,[66] the biexponential decay kinetics might result from conformations containing different pyridyl-stilbene dihedral angles (Figure 6b). In principle, increasing the pryidyl-stilbene torsion angle would lead to a larger extent of charge separation, more polar excited states, and longer fluorescence decay times (τ_f). Thus, the longer fluorescence lifetime observed in MeCN vs hexane might suggest that the long-lived component is due to conformers of a larger pyridyl-stilbene torsion angle. Nevertheless, the fact of $\Phi_f + 2\Phi_{tc} \approx 1.0$ suggests that the torsion angle is insufficiently large to form a distinct TICT state that quenches the excited state without undergoing *trans* → *cis* isomerization as seen for some *trans*-aminostilbenes in polar solvents.[58,66,79] The single exponential decay kinetics observed for the other three ligands is consistent with the scenario of aminostilbene- or aminostilbazole-localized CT states indicated by solvatofluorochromism and DFT calculations.

Table 4 also shows the rate constant for fluorescence ($k_f = \Phi_f/\tau_f$) and the overall nonradiative deactivation processes ($k_{nr} = (1 - \Phi_f)/\tau_f$). Since increasing the solvent polarity results in a larger decrease in the nonradiative decay constant (k_{nr}) than the fluorescent rate constant (k_f) (vide infra), the solvent effect on Φ_f and Φ_{tc} could be again attributed to perturbations of the C═C torsion barrier, which is larger in more polar solvents.

Excited-State Behavior of the Pt Complexes. Emission spectra of the Pt complexes were recorded in solutions at room temperature and in a 2-methyltetrahydrofuran (MTHF) solvent glass at 77 K (Figure 8). The photoluminescence quantum efficiency is rather low (<0.001) for all four complexes, as observed for **C1-Et**,[60] in degassed DCM at room temperature. The relative emission maximum reflects qualitatively their relative strength of ILCT as discussed above based on their absorption spectra (Figure 2b). The weak emission of **C1-Et** was attributed to the Pt(ppy)(acac) moiety in a conformation of a half-twisted C═C bond (i.e., the phosphorescence of the $^3p^*$ state of the complex).[60] However, the observed emission is more likely fluorescence rather than phosphorescence, as the emission wavelength is similar to that of the corresponding ligands and a $^3p^*$ state should not be emissive. The photoluminescence is enhanced in a MTHF glass at 77 K, and the emission spectra consist of two distinct spectral profiles located at regions of 450−600 nm and above 600 nm. The short-wavelength emission is located in the same region as the room-temperature fluorescence, and the long-wavelength emission, which is not observed at room temperature, displays well-defined vibrational structures. We assigned the short- and long-wavelength emissions to fluorescence and phosphorescence, respectively. Phosphorescence has been observed for many Pt complexes[1−10,80] as a result of the heavy Pt atom that facilitates the $S_1 \rightarrow T_1$ (or T_n) intersystem crossing. The long lifetimes of 39−64 μs for the long-wavelength emission indeed support this assignment. The significantly longer phosphorescence lifetime for **C1-Me** (64 μs) than the others (39−43 μs) is worth noting. It might reflect a larger CT character in T_1. The phosphorescence spectra of all four cases are independent of the excitation wavelengths. The wavelength of the 0−0 phosphorescence band is **C1-Ph** > **C1-Me** > **C2-Ph** > **C2-Me**, although the difference is rather small. This order is the same as that of λ_{abs} for the corresponding ligands (**L1-Ph** > **L1-Me** > **L2-Ph** > **L2-Me**), which indicates that the styryl position and the *N*-phenyl conjugation effects are also in operation but to a much lesser extent. This again suggests that the T_1 state of **C1** and **C2** systems is mainly localized on the *trans*-stilbazole and *trans*-stilbene moiety, respectively. The phenomenon of a more localized T_1 state than the S_1 state was also observed for other platinum complexes.[59]

As shown in Table 5, the triplet energy (E_T) and phosphorescence maxima (λ_p) for the Pt complexes resemble

Table 5. Triplet Energy (E_T), Phosphorescence Peak Maxima (λ_p), and Difference between the 0−0 and 0−1 Bands ($\Delta\nu_{vib}$) for the Pt Complexes and NMS in a MTHF Glass at 77 K

compd	E_T[a] (kcal/mol)	λ_p (nm)	$\Delta\nu_{vib}$[b] (cm^{-1})	τ_p (μs)
C1-Me	44.4	645, 711	1439	64
C1-Ph	44.3	646, 715	1494	39
C2-Me	46.1	623, 690	1559	41
C2-Ph	45.6	628, 696	1556	43
NMS[c]	45.2	632, 690	1330	

[a]The E_T value was calculated from the 0−0 band. [b]Deduced from the phosphorescence 0−0 and 0−1 bands. [c]Data were taken from ref 81.

dx.doi.org/10.1021/jp304893c | J. Phys. Chem. B 2012, 116, 8222−8232

those of *trans*-4-nitro-4′-methoxystilbene (NMS),[81] a push−pull *trans*-stilbene. It is noted that the vibronic energy ($\Delta\nu_{vib}$), as deduced from the 0−0 and 0−1 bands, is 100−200 cm^{-1} larger for the Pt complexes than NMS.

Like the ligands, the *trans* → *cis* photoisomerization takes place for all four Pt complexes (Figure 7). The Φ_{tc} values are near 0.50 for all cases at room temperature (Table 4). With the facts of no phosphorescence and $2\Phi_{tc} \sim 1.0$, we conclude that the C═C torsion in T_1 is likely a barrierless process, conforming to the OBT isomerization PES for *trans*-stilbene (Figure 1). This is reminiscent of the results reported by Schanze et al. for the complex *trans*-$(PPh_3)_2Pt(—C{\equiv}C—t\text{-}St)_2$ in toluene, which has a Φ_{tc} value of 0.42, roughly half of the quantum efficiency for intersystem crossing ($\Phi_{isc} = 0.75 \pm 0.05$).[59]

When the solutions of the complexes are saturated with molecular oxygen, a decrease in Φ_{tc} was observed. For example, the Φ_{tc} value is lowered by 12 and 34% for **C1-Me** and **C1-Ph**, respectively, in aerated DCM as compared to that in degassed DCM. The molecular oxygen effect on Φ_{tc} was reported to be ca. 8 ± 5% for the triplet-sensitized isomerization of *trans*-stilbene.[82,83] A higher sensitivity for the Φ_{tc} of the Pt complexes vs *trans*-stilbene to molecular oxygen might reflect the relative efficiency of the T_1 formation, which is more efficient through Pt-mediated intramolecular spin−orbit couplings vs intermolecular triplet energy transfer.

CONCLUSION

We have investigated and compared the photophysical and photochemical properties of four *trans*-aminostyrene-conjugated phenylpyridine C^N ligands and their cyclometalated Pt(II)(acac) complexes. The results show that both the styryl position and the *N*-phenyl substituent effects on photoluminescence and *trans* → *cis* photoisomerization are significant for the free ligands but small or negligible for the Pt complexes, although the excited state of the complexes is dominated by the C^N ligands. The distinct quantum efficiency in photoisomerization between the free ligands and the Pt complexes mainly results from the nature of the operated excited states, which is S_1 for the free ligands but T_1 for the Pt complexes. Nevertheless, the free ligands and the Pt complexes exhibit a common feature of $\Phi_f + 2\Phi_{tc} \approx 1.0$ in solutions at room temperature. All these observations could be understood in terms of the one-bond-twist photoisomerization mechanism deduced for *trans*-stilbenes and *trans*-aminostilbenes; namely, ca. 50% of the C═C torsion leads to formation of the *cis* isomers, and the process of the C═C bond torsion encounters a thermal barrier in S_1 but is essentially barrierless in T_1.[46,47,55,84] The presence of a substituent- and solvent-dependent barrier for the C═C torsion in S_1 but not in T_1 accounts for the strong fluorescence for the free ligands and the absence of phosphorescence for the Pt complexes. Therefore, C^N ligands containing the aminostilbene and aminostilbazole moiety are ideal ligands to create Pt complexes of high *trans*−*cis* photoisomerization efficiency for applications in photochromic systems or light-driven molecular switches. On the other hand, C^N ligands having the moiety of aminostilbene and aminostilbazole should be avoided if high photoluminescence of their Pt complexes is desired for the purpose of being optical probes or light-emitting materials.

EXPERIMENTAL SECTION

Materials. Solvents for spectra and quantum yield measurement were all HPLC grade and used as received. THF and MTHF were dried by sodium metal and distilled before used. All the new compounds were identified by ^1H NMR and ^{13}C NMR spectroscopy, mass spectrometry, and/or element analysis.

Methods. Electronic spectra were recorded at room temperature (23 ± 1 °C). UV−visible spectra were measured by using a Cary300 double beam spectrophotometer. Fluorescence spectra were recorded by using a PTI QuantaMaster C-60 or the Edinburgh FLS920 spectrometers and corrected for the response of the detector. The optical density (OD) of all solutions was about 0.1 at the wavelength of excitation. A N_2-outgassed (5 min) solution of anthracene (λ_{ex} = 355 nm, Φ_f = 0.27 in hexane)[85] and a N_2-outgassed (10 min) solution of 9,10-diphenylanthracene (λ_{ex} = 371 nm, Φ_f = 0.93 in hexane)[86] were used as standards for the fluorescence quantum yield determinations of compounds under N_2-outgassed solutions with solvent refractive index correction. An error of 10% is estimated for the fluorescence quantum yields. Fluorescence decays were measured at room temperature by using an Edinburgh FLS920 spectrometer with a gated hydrogen arc lamp using a scatter solution to profile the instrument response function. Corrected phosphorescence spectra were recorded at 77 K in an EPR tube with a Cold Finger Dewars Flask in a Edinburgh FLS920 spectrometer with a R928 detector. Phosphorescence decays were measured at 77 K by means of the Edinburgh FLS920 spectrometer apparatus with a μF900 lamp using self-scattering to profile the instrument response function. The μF900 is a pulsed xenon flashlamp that can be used to measure decays from 1.5 μs to 10 s within the pulse duration between 1.5 to 2.5 μs. The goodness of nonlinear least-squares fit for both fluorescence and phosphorescence decays was judged by the reduced χ^2 value (<1.2 in all cases), the randomness of the residuals, and the autocorrelation function. Quantum yields of photoisomerization were measured on optically dense degassed solutions (10^{-3}−10^{-4} M) at 350 or 381 nm using a 75 W Xe arc lamp and monochromator. 4-(*N*-Phenylamino)stilbene (λ_{ex} = 350 nm, Φ_{tc} = 0.34 in DCM)[58] and 4-cyano-4′-(*N*-methyl-*N*-phenylamino)stilbene (λ_{ex} = 381 nm, Φ_{tc} = 0.37 in DCM)[65] were used as reference standards. The extent of photoisomerization (<10%) was determined using HPLC analysis (Waters 600 Controller and 996 photodiode array detector, Thermo APS-2 Hypersil, hexane, THF, and ethyl acetate mixed solvent) without back-reaction corrections. The reproducibility error was <10% of the average. Density functional theory (DFT) calculations were performed using the Gaussian 09 program[87] package at the B3LYP[69−71] level for ligands. For complexes, the Stuttgart−Dresden (SDD)[73] basis set was used with a relativistic effective core potential for Pt, and all ligand atoms (C, H, N, and O) were described by the Cam-B3LYP[72] 6-31G(d,p) basis set. Singlet and triplet excitation energies were calculated by time-dependent DFT (TD-DFT) at optimized geometries, and the solvents were described by the CPCM polarizable conductor calculation model.[88,89] The optimized ground state geometries of ligands and complexes were investigated by varying the dihedral angle between every four atoms except for hydrogen atoms. TD-DFT calculation was used to calculate six lowest singlet and triplet transitions, respectively.

dx.doi.org/10.1021/jp304893c | J. Phys. Chem. B 2012, 116, 8222−8232

■ ASSOCIATED CONTENT

Supporting Information

Synthetic scheme and procedures and compound characterization data for the ligands and complexes, crystal structures of **L2-Ph** and **C2-Ph**, structural details of DFT-calculated complexes, complete reference 87, FMOs of the ligands and complexes, UV−vis absorption titration spectra of **L1-Me** in large excess of HCl, and DFT-derived Cartesian coordinates for the ligands and complexes. This material is available free of charge via the Internet at http://pubs.acs.org.

■ AUTHOR INFORMATION

Corresponding Author

*E-mail: jsyang@ntu.edu.tw.

Notes

The authors declare no competing financial interest.

■ ACKNOWLEDGMENTS

We thank National Taiwan University (Excellent Research Project 10R80912-3) and the National Science Council of Taiwan, ROC, for financial support. The computing time granted by the Computing Center of NTU is also acknowledged.

■ REFERENCES

(1) Lu, W.; Mi, B.-X.; Chan, M. C. W.; Hui, Z.; Che, C.-M.; Zhu, N.; Lee, S.-T. *J. Am. Chem. Soc.* **2004**, *126*, 4958−4971.
(2) Norel, L.; Rudolph, M.; Vanthuyne, N.; Williams, J. A. G.; Lescop, C.; Roussel, C.; Autschbach, J.; Crassous, J.; Réau, R. *Angew. Chem., Int. Ed.* **2010**, *49*, 99−102.
(3) Macchi, G.; Meinardi, F.; Tubino, R. *Adv. Mater.* **2010**, *22*, 3553−3557.
(4) Komiya, N.; Muraoka, T.; Iida, M.; Miyanaga, M.; Takahashi, K.; Naota, T. *J. Am. Chem. Soc.* **2011**, *133*, 16054−16061.
(5) Yersin, H.; Rausch, A. F.; Czerwieniec, R.; Hofbeck, T.; Fischer, T. *Coord. Chem. Rev.* **2011**, *255*, 2622−2652.
(6) Graham, K. R.; Yang, Y.; Sommer, J. R.; Shelton, A. H.; Schanze, K. S.; Xue, J.; Reynolds, J. R. *Chem. Mater.* **2011**, *23*, 5305−5312.
(7) Rausch, A. F.; Murphy, L.; Williams, J. A. G.; Yersin, H. *Inorg. Chem.* **2012**, *51*, 312−319.
(8) Zhou, G.; Wong, W.-Y.; Yang, X. *Chem.—Asian J.* **2011**, *6*, 1706−1727.
(9) Kalinowski, J.; Fattori, V.; Cocchi, M.; Williams, J. A. G. *Coord. Chem. Rev.* **2011**, *255*, 2401−2425.
(10) Kui, S. C. F.; Hung, F.-F.; Lai, S.-L.; Yuen, M.-Y.; Kwok, C.-C.; Low, K.-H.; Chui, S. S.-Y.; Che, C.-M. *Chem.—Eur. J.* **2012**, *18*, 96−109.
(11) Sakamoto, R.; Kume, S.; Sugimoto, M.; Nishihara, H. *Chem.—Eur. J.* **2009**, *15*, 1429−1439.
(12) Brayshaw, S. K.; Schiffers, S.; Stevenson, A. J.; Teat, S. J.; Warren, M. R.; Bennett, R. D.; Sazanovich, I. V.; Buckley, A. R.; Weinstein, J. A.; Raithby, P. R. *Chem.—Eur. J.* **2011**, *17*, 4385−4395.
(13) Demas, J. N.; DeGraff, B. A. *Coord. Chem. Rev.* **2001**, *211*, 317−351.
(14) Lanoë, P.-H.; Fillaut, J.-L.; Toupet, L.; Williams, J. A. G.; Le Bozec, H.; Guerchais, V. *Chem. Commun.* **2008**, 4333−4335.
(15) Tian, Y.; Shumway, B. R.; Meldrum, D. R. *Chem. Mater.* **2010**, *22*, 2069−2078.
(16) Lanoë, P.-H.; Le Bozec, H.; Williams, J. A. G.; Fillaut, J.-L.; Guerchais, V. *Dalton Trans.* **2010**, *39*, 707−710.
(17) Wu, W.; Wu, W.; Ji, S.; Guo, H.; Song, P.; Han, K.; Chi, L.; Shao, J.; Zhao, J. *J. Mater. Chem.* **2010**, *20*, 9775−9786.
(18) Liu, Y.; Guo, H.; Zhao, J. *Chem. Commun.* **2011**, *47*, 11471−11473.
(19) Guerchais, V.; Fillaut, J.-L. *Coord. Chem. Rev.* **2011**, *255*, 2448−2457.
(20) Santoro, A.; Whitwood, A. C.; Williams, J. A. G.; Kozhevnikov, V. N.; Bruce, D. W. *Chem. Mater.* **2009**, *21*, 3871−3882.
(21) Vezzu, D. A. K.; Ravindranathan, D.; Garner, A. W.; Bartolotti, L.; Smith, M. E.; Boyle, P. D.; Huo, S. *Inorg. Chem.* **2011**, *50*, 8261−8273.
(22) Mou, X.; Wu, Y.; Liu, S.; Shi, M.; Liu, X.; Wang, C.; Sun, S.; Zhao, Q.; Zhou, X.; Huang, W. *J. Mater. Chem.* **2011**, *21*, 13951−13962.
(23) Brooks, J.; Babayan, Y.; Lamansky, S.; Djurovich, P. I.; Tsyba, I.; Bau, R.; Thompson, M. E. *Inorg. Chem.* **2002**, *41*, 3055−3066.
(24) Karthaus, O.; Ueda, K.; Yamagishi, A.; Shimomura, M. *J. Photochem. Photobiol., A* **1995**, *92*, 117−120.
(25) Coe, B. J.; Hamor, T. A.; Jones, C. J.; McCleverty, J. A.; Bloor, D.; Cross, G. H.; Axon, T. L. *J. Chem. Soc., Dalton Trans.* **1995**, 673−684.
(26) Coe, B. J.; Harris, J. A.; Brunschwig, B. S.; Garin, J.; Orduna, J.; Coles, S. J.; Hursthouse, M. B. *J. Am. Chem. Soc.* **2004**, *126*, 10418−10427.
(27) Kang, H.; Facchetti, A.; Jiang, H.; Cariati, E.; Righetto, S.; Ugo, R.; Zuccaccia, C.; Macchioni, A.; Stern, C. L.; Liu, Z.; Ho, S.-T.; Brown, E. C.; Ratner, M. A.; Marks, T. J. *J. Am. Chem. Soc.* **2007**, *129*, 3267−3286.
(28) Feuvrie, C.; Maury, O.; Le Bozec, H.; Ledoux, I.; Morrall, J. P.; Dalton, G. T.; Samoc, M.; Humphrey, M. G. *J. Phys. Chem. A* **2007**, *111*, 8980−8985.
(29) Vijayakumar, T.; Hubert Joe, I.; Reghunadhan Nair, C. P.; Jayakumar, V. S. *Chem. Phys.* **2008**, *343*, 83−99.
(30) Yu, G.; Gao, J.; Hummelen, J. C.; Wudl, F.; Heeger, A. J. *Science* **1995**, *270*, 1789−1791.
(31) Hwang, D.-H.; Kim, S. T.; Shim, H.-K.; Holmes, A. B.; Moratti, S. C.; Friend, R. H. *Chem. Commun.* **1996**, 2241−2242.
(32) Hide, F.; DÍaz-GarcÍa, M. A.; Schwartz, B. J.; Heeger, A. J. *Acc. Chem. Res.* **1997**, *30*, 430−436.
(33) Friend, R. H.; Gymer, R. W.; Holmes, A. B.; Burroughes, J. H.; Marks, R. N.; Taliani, C.; Bradley, D. D. C.; Santos, D. A. D.; Brédas, J. L.; Lögdlund, M.; Salaneck, W. R. *Nature* **1999**, *397*, 121−128.
(34) Mitschke, U.; Bäuerle, P. *J. Mater. Chem.* **2000**, *10*, 1471−1507.
(35) Zhao, C.-H.; Wakamiya, A.; Inukai, Y.; Yamaguchi, S. *J. Am. Chem. Soc.* **2006**, *128*, 15934−15935.
(36) Traub, M. C.; Lakhwani, G.; Bolinger, J. C.; Bout, D. V.; Barbara, P. F. *J. Phys. Chem. B* **2011**, *115*, 9941−9947.
(37) Stanier, C. A.; Alderman, S. J.; Claridge, T. D. W.; Anderson, H. L. *Angew. Chem., Int. Ed.* **2002**, *41*, 1769−1772.
(38) Yang, J.-S.; Huang, Y.-T.; Ho, J.-H.; Sun, W.-T.; Huang, H.-H.; Lin, Y.-C.; Huang, S.-J.; Huang, S.-L.; Lu, H.-F.; Chao, I. *Org. Lett.* **2008**, *10*, 2279−2282.
(39) Rurack, K.; Rettig, W.; Resch-Genger, U. *Chem. Commun.* **2000**, 407−408.
(40) Simeonov, A.; Matsushita, M.; Juban, E. A.; Thompson, E. H. Z.; Hoffman, T. Z.; Beuscher, A. E., IV; Taylor, M. J.; Wirsching, P.; Rettig, W.; McCusker, J. K.; Stevens, R. C.; Millar, D. P.; Schultz, P. G.; Lerner, R. A.; Janda, K. D. *Science* **2000**, *290*, 307−313.
(41) Yang, J.-S.; Lin, Y.-D.; Lin, Y.-H.; Liao, F.-L. *J. Org. Chem.* **2004**, *69*, 3517−3525.
(42) Debler, E. W.; Kaufmann, G. F.; Meijler, M. M.; Heine, A.; Mee, J. M.; Pljevaljčić, G.; Di Bilio, A. J.; Schultz, P. G.; Millar, D. P.; Janda, K. D.; Wilson, I. A.; Gray, H. B.; Lerner, R. A. *Science* **2008**, *319*, 1232−1235.
(43) Huang, C.; Fan, J.; Peng, X.; Lin, Z.; Guo, B.; Ren, A.; Cui, J.; Sun, S. *J. Photochem. Photobiol., A* **2008**, *199*, 144−149.
(44) Vijayakumar, C.; Tobin, G.; Schmitt, W.; Kim, M.-J.; Takeuchi, M. *Chem. Commun.* **2010**, *46*, 874−876.
(45) Körsten, S.; Mohr, G. J. *Chem.—Eur. J.* **2011**, *17*, 969−975.
(46) Waldeck, D. H. *Chem. Rev.* **1991**, *91*, 415−436.
(47) Kovalenko, S. A.; Dobryakov, A. L.; Ioffe, I.; Ernsting, N. P. *Chem. Phys. Lett.* **2010**, *493*, 255−258.
(48) Saltiel, J.; Charlton, J. L. In *Rearrangements in Ground and Excited States*; de Mayo, P., Ed.; Academic Press: New York, 1980; Vol. 3, pp 25−89.

(49) Saltiel, J.; Sun, Y.-P. In *Photochromism, Molecules and Systems*; Dürr, H., Bouas-Laurent, H., Eds.; Elsevier: Amsterdam, 1990; pp 64−164.
(50) Meier, H. *Angew. Chem., Int. Ed. Engl.* **1992**, *31*, 1399−1420.
(51) Gőrner, H.; Kuhn, H. J. *Adv. Photochem.* **1995**, *19*, 1−117.
(52) Lewis, F. D.; Yang, J.-S. *J. Am. Chem. Soc.* **1997**, *119*, 3834−3835.
(53) Lewis, F. D.; Kalgutkar, R. S.; Yang, J.-S. *J. Am. Chem. Soc.* **1999**, *121*, 12045−12053.
(54) Yang, J.-S.; Chiou, S.-Y.; Liau, K.-L. *J. Am. Chem. Soc.* **2002**, *124*, 2518−2527.
(55) Lin, C.-K.; Prabhakar, C.; Yang, J.-S. *J. Phys. Chem. A* **2011**, *115*, 3233−3242.
(56) Bartocci, G.; Mazzucato, U.; Masetti, F.; Galiazzo, G. *J. Phys. Chem.* **1980**, *84*, 847−851.
(57) Mazzucato, U. *Pure Appl. Chem.* **1982**, *54*, 1705−1721.
(58) Yang, J.-S.; Liau, K.-L.; Wang, C.-M.; Hwang, C.-Y. *J. Am. Chem. Soc.* **2004**, *126*, 12325−12335.
(59) Haskins-Glusac, K.; Ghiviriga, I.; Abboud, K. A.; Schanze, K. S. *J. Phys. Chem. B* **2004**, *108*, 4969−4978.
(60) Yin, B.; Niemeyer, F.; Williams, J. A. G.; Jiang, J.; Boucekkine, A.; Toupet, L.; Le Bozec, H.; Guerchais, V. *Inorg. Chem.* **2006**, *45*, 8584−8596.
(61) Batema, G. D.; van de Westelaken, K. T. L.; Guerra, J.; Lutz, M.; Spek, A. L.; van Walree, C. A.; Donegá, C. d. M.; Meijerink, A.; van Klink, G. P. M.; van Koten, G. *Eur. J. Inorg. Chem.* **2007**, 1422−1435.
(62) Batema, G. D.; Lutz, M.; Spek, A. L.; van Walree, C. A.; Donegá, C. d. M.; Meijerink, A.; Havenith, R. W. A.; Pérez-Moreno, J.; Clays, K.; Büchel, M.; Dijken, A. v.; Bryce, D. L.; van Klink, G. P. M.; van Koten, G. *Organometallics* **2008**, *27*, 1690−1701.
(63) Baik, C.; Wang, S. *Chem. Commun.* **2011**, *47*, 9432−9434.
(64) Yang, J.-S.; Wang, C.-M.; Hwang, C.-Y.; Liau, K.-L.; Chiou, S.-Y. *Photochem. Photobiol. Sci.* **2003**, *2*, 1225−1231.
(65) Yang, J.-S.; Liau, K.-L.; Tu, C.-W.; Hwang, C.-Y. *J. Phys. Chem. A* **2005**, *109*, 6450−6456.
(66) Yang, J.-S.; Liau, K.-L.; Li, C.-Y.; Chen, M.-Y. *J. Am. Chem. Soc.* **2007**, *129*, 13183−13192.
(67) Dieck, H. A.; Heck, R. F. *J. Am. Chem. Soc.* **1974**, *96*, 1133−1136.
(68) Heck, R. F. *Acc. Chem. Res.* **1979**, *12*, 146−151.
(69) Becke, A. D. *Phys. Rev. A* **1988**, *38*, 3098−3100.
(70) Lee, C.; Yang, W.; Parr, R. G. *Phys. Rev. B* **1988**, *37*, 785−789.
(71) Miehlich, B.; Savin, A.; Stoll, H.; Preuss, H. *Chem. Phys. Lett.* **1989**, *157*, 200−206.
(72) Yanai, T.; Tew, D. P.; Handy, N. C. *Chem. Phys. Lett.* **2004**, *393*, 51−57.
(73) Andrae, D.; Häußermann, U.; Dolg, M.; Stoll, H.; Preuß, H. *Theor. Chem. Acc.* **1990**, *77*, 123−141.
(74) Kobayashi, S.; Busujima, T.; Nagayama, S. *Chem.—Eur. J.* **2000**, *6*, 3491−3494.
(75) Maury, O.; Guégan, J.-P.; Renouard, T.; Hilton, A.; Dupau, P.; Sandon, N.; Toupet, L.; Le Bozec, H. *New J. Chem.* **2001**, *25*, 1553−1566.
(76) Detert, H.; Lehmann, M.; Meier, H. *Materials* **2010**, *3*, 3218−3330.
(77) *CRC Handbook of Chemistry and Physics*, 92nd ed.; CRC Press: 2011−2012.
(78) Petkova, I.; Dobrikov, G.; Banerji, N.; Duvanel, G.; Perez, R.; Dimitrov, V.; Nikolov, P.; Vauthey, E. *J. Phys. Chem. A* **2010**, *114*, 10−20.
(79) Yang, J.-S.; Liau, K.-L.; Hwang, C.-Y.; Wang, C.-M. *J. Phys. Chem. A* **2006**, *110*, 8003−8010.
(80) Chou, P.-T.; Chi, Y.; Chung, M.-W.; Lin, C.-C. *Coord. Chem. Rev.* **2011**, *255*, 2653−2665.
(81) Görner, H. *J. Phys. Chem.* **1989**, *93*, 1826−1832.
(82) Garner, A.; Wilkinson, F. In *Singlet Oxygen, Reaction With Organic Compounds and Polymers*; Ranby, B., Rabek, J. F., Eds.; Wiley: New York, 1976; pp 48−53.
(83) Saltiel, J.; Klima, R. F. *Photochem. Photobiol.* **2006**, *82*, 38−42.
(84) Takeuchi, S.; Ruhman, S.; Tsuneda, T.; Chiba, M.; Taketsugu, T.; Tahara, T. *Science* **2008**, *322*, 1073−1077.
(85) Dawson, W. R.; Windsor, M. W. *J. Phys. Chem.* **1968**, *72*, 3251−3260.
(86) Meech, S. R.; Phillips, D. *J. Photochem.* **1983**, *23*, 193−217.
(87) Frisch, M. J.; et al. *Gaussian 09*, revision A.02; Gaussian, Inc.: Wallingford CT, 2009.
(88) Barone, V.; Cossi, M. *J. Phys. Chem. A* **1998**, *102*, 1995−2001.
(89) Cossi, M.; Rega, N.; Scalmani, G.; Barone, V. *J. Comput. Chem.* **2003**, *24*, 669−681.